

Temperature as an external field for colloid-polymer mixtures : “quenching” by heating and “melting” by cooling

Shelley L. Taylor

School of Chemistry, University of Bristol, Bristol, BS8 1TS, UK.

Robert Evans

H.H. Wills Physics Laboratory, University of Bristol, Bristol, BS8 1TL, UK.

C. Patrick Royall

School of Chemistry, University of Bristol, Bristol, BS8 1TS, UK.

E-mail: paddy.royall@bristol.ac.uk

Received April 20th, 2012

Abstract. We investigate the response to temperature of a well-known colloid-polymer mixture. At room temperature, the critical value of the second virial coefficient of the effective interaction for the Asakura-Oosawa model predicts the onset of gelation with remarkable accuracy. Upon cooling the system, the effective attractions between colloids induced by polymer depletion are reduced, because the polymer radius of gyration decreases as the θ -temperature is approached. Paradoxically, this raises the effective temperature, leading to “melting” of colloidal gels. We find the Asakura-Oosawa model of effective colloid interactions with a simple description of the polymer temperature response provides a quantitative description of the fluid-gel transition. Further we present evidence for enhancement of crystallisation rates near the metastable critical point.

1. Introduction

Colloid-polymer mixtures occupy a special place in soft matter physics [1, 2]. The introduction of non-adsorbing polymer introduces an effective attraction between the colloids whose strength and range can be tuned by altering the concentration and molecular weight, respectively, of the polymer [2, 3, 4, 5, 6]. The existence of this entropy driven depletion attraction opens up a vast swathe of behaviour inaccessible to colloidal systems with purely repulsive interactions, such that colloid-polymer mixtures may be regarded as true “model atomic systems” [1]. The best known examples include liquid-gas phase separation [1, 2] but there are also phenomena not seen in atomic systems such as gelation [1] and re-entrant glassy dynamics at high density [7]. Real-space

analysis at the particle level has enabled direct observation of crystallisation [8], and behaviour related to liquid-gas phase separation such as capillary wave fluctuations at (colloidal) liquid-gas interfaces [9] and fluid critical phenomena [10]. Moreover colloid-polymer mixtures with a relatively short-ranged attractive interaction can (crudely) model proteins and may exhibit two-step crystal nucleation phenomena [11], to which we return below.

Theoretical treatments of colloid-polymer mixtures are based largely on the Asakura-Oosawa-Vrij (AO) model [3, 4, 6] which treats the colloid-colloid interaction as that of hard-spheres (HS) and the polymer-polymer interaction as ideal, i.e. the polymer coils are assumed to be perfectly interpenetrating spheres. However, the polymer spheres have an excluded volume (hard) interaction with the HS colloids. This model binary (AO) mixture provides the simplest, zeroth-order description of the real mixture. It is characterized by the size ratio $q = \sigma_p/\sigma$, where σ is the colloid diameter and σ_p is the polymer sphere diameter. The colloid-polymer interaction is infinite for separations $r < (\sigma + \sigma_p)/2$. From simulation and theoretical studies it is well-known that for sufficiently large size ratios, $q \gtrsim 0.3$, the AO model exhibits phase separation into a colloid-rich (liquid) and a colloid-poor (gas) phase at sufficiently high polymer volume fractions. For smaller size ratios this phase transition becomes metastable w.r.t. the fluid-crystal transition [12, 13, 14]. The same trend in phase behaviour (with σ_p set equal to twice the radius of gyration of the non-adsorbing polymer) is found in experimental studies [15, 1, 2]. In addition to predicting purely entropy driven fluid-fluid phase separation the AO model exhibits the elegant feature that for size ratios $q < (2/\sqrt{3} - 1) = 0.1547$ the degrees of freedom of the ideal polymer can be integrated out exactly and the binary mixture maps formally to a one-component system of colloids described by an effective Hamiltonian containing only one and two-body (pair) contributions [12, 14]. The former contribution plays no role in determining phase equilibrium or structure, for a uniform (bulk) fluid, but does determine the total pressure and compressibility [16]. The pair interaction between the HS colloids, given by integrating out the ideal polymer, is the standard AO potential:

$$\beta u_{AO}(r) = \begin{cases} \infty & \text{for } r < \sigma \\ -\phi_p \frac{(1+q)^3}{q^3} & \\ \times \left[1 - \frac{3r}{2(1+q)\sigma} + \frac{r^3}{2(1+q)^3\sigma^3} \right] & \text{for } \sigma < r < \sigma + \sigma_p \\ 0 & \text{for } r > \sigma + \sigma_p \end{cases} \quad (1)$$

β is $1/k_B T$ where k_B is Boltzmann’s constant and T is temperature. Since the analysis is performed in the semi-grand ensemble the polymer volume fraction in the reservoir $\phi_p = \pi \sigma_p^3 z_p / 6$ appears in Eq. (vrefeqAO). The polymer fugacity z_p is equal to the number density ρ_p of ideal polymers in the reservoir at the given chemical potential μ_p . As noted already, in relating the AO model to experiment, one usually sets $\sigma_p = 2R_G$ where R_G is the polymer radius of gyration. Hitherto, most work on colloidal-polymer mixtures

was carried out at a fixed temperature, typically around 25 °C. *Effective* temperature is varied by changing the interaction strength. The effective temperature is inversely proportional to the depth of the attractive well of the interaction potential in (Eq. 1), and is therefore fixed for a given polymer reservoir density. Scanning a phase diagram then requires preparation of a considerable number of different samples. Conversely, in molecular systems, interactions are usually constant over the (broad) temperature range of interest, one sample is prepared and temperature is used as a control parameter.

In our present study we note that colloid-polymer mixtures can respond to temperature in an intriguing and counter-intuitive manner. The effective temperature in Eq. (1) is set by z_p which in turn is equal to the polymer number density for ideal polymers. Real systems approximate this behaviour very well [17]. Thus the primary response of the system to temperature is given by the response of the polymer depletant, since the polymer-polymer interactions are weak and colloid-colloid interactions are athermal (hard sphere). Now, close to (but above) their theta temperature T^θ , polymers expand (R_G increases) upon heating (Fig. 1) . This expansion has two effects : firstly, the polymer-colloid size ratio q increases, thereby increasing the range of attraction, and secondly, the polymer reservoir volume fraction $\phi_p = \pi\rho_p\sigma_p^3/6$ also increases. Since the well-depth $-\beta u_{AO}(\sigma) = \pi\rho_p\sigma^3q^2(1 + \frac{2}{3}q)/4$ this means the effective temperature falls strongly for a modest increase in polymer size which leads to a paradoxical result, namely raising the temperature of a colloid-polymer mixture near T^θ brings about a strong *effective cooling*. Although this effect has been exploited to drive phase transitions in mixtures of colloidal rods and polymers [18], these temperature-dependent depletion interactions have received relatively little attention. This is in contrast to other means of controlling the attractive interactions between colloids in-situ, such as the critical Casimir effect[19, 20, 21] and multiaxial electric fields [22]. We note that in-situ control of attractive interactions, combined with particle-resolved studies, has the power to provide much new insight into a variety of phenomena, including phase transitions [23].

Here we make a quantitative experimental investigation, at the single-particle level, of the effect of temperature on an already well-studied colloid-polymer mixture. The elucidation of our results requires theoretical underpinning and we shall base this on the AO model described above. Specifically we investigate a mixture where the size ratio is about 0.2 but varies by 10 percent or so on changing temperature. The size ratio is such that the fluid-fluid transition is metastable w.r.t. the fluid-solid transition and therefore we consider out of equilibrium phenomena associated with metastable states. A recent simulation study [24] provides a helpful framework for placing our results in context. These authors study the effective one-component AO model, where the pair-potential is given by Eq(1), for $q = 0.15$ which is in the regime where the mapping to the effective one-component description using only a pair potential is exact. By changing the polymer reservoir density , equivalent to changing the depth of the attractive potential well, they determine both equilibrium and out-of equilibrium phase diagrams. More specifically, using Monte Carlo and Brownian dynamics, they investigate crystal nucleation and the onset of gelation in the vicinity of the metastable fluid-fluid binodal. They present

convincing evidence that crystallization is enhanced by the binodal. We tackle the same issues in our experiments on a real colloid-polymer mixture, seeking to ascertain what role proximity to the binodal plays in forming gels and in determining crystal nucleation rates.

It is well-known that in experiments equilibrium is often not reached and in particular gelation can occur. This phenomenon has been linked to spinodal decomposition associated with colloidal gas-liquid condensation [25, 26]; gels are supposed to form within the metastable fluid-fluid spinodal. It follows that knowledge of the critical point is important in predicting where gelation might occur [26].

The connection between critical density fluctuations and crystal nucleation rates in short-ranged attractive systems, where the gas-liquid critical point is metastable with respect to crystallisation, has received considerable attention since it was elucidated by Ten Wolde and Frenkel [27]. Critical fluctuations are expected to enhance the nucleation rate and may be responsible for the strong temperature dependence of nucleation rates found in globular proteins [28, 29]. A two-step nucleation process is envisaged where nuclei preferentially form in fluctuations of high density since the surface tension between the nucleus and the surrounding fluid is smaller. The reduction in free energy barrier to nucleation associated with such density fluctuations has been measured in a 2D depletion system [11]. Here we investigate crystallisation in the neighbourhood of the metastable critical point.

This paper is organised as follows. In section 2 we first introduce the experimental system, and discuss the response of the polymer component to temperature. We then discuss relating experiment and theory in terms of the AO model. In section 3 we present results for (i) the room-temperature phase diagram, (ii) crystallisation around the metastable critical point and (iii) the response of the system to temperature. We conclude in section 4.

2. Methods

2.1. Experimental

Our experimental system is based on polymethyl methacrylate (PMMA) colloids. The colloid diameter $\sigma = 1080$ nm with polydispersity 4.6%, as determined from static light scattering. The polystyrene polymer used has a molecular weight $M_w = 8.5 \times 10^6$, which corresponds to a radius of gyration of $R_G^\theta = 95$ nm under θ conditions [31]. This leads to a polymer-colloid size ratio of $q(T = T^\theta) = 0.176$. The colloids and polymer are dispersed in a solution of *cis* decalin, where we find T^θ of polystyrene is 10°C . We image this system at the single particle level with a Leica SP5 confocal microscope. To this microscope we have fitted a temperature stage which uses a Peltier chip to cool from room temperature (25°C) to the θ -temperature and below. Note that our experimental system is not density-matched. The gravitational length $\lambda_g = k_B T / (mg) = 1.96\sigma$, where m is the buoyant mass of the colloid and g is the acceleration due to gravity.

Sedimentation therefore becomes an issue at long times, limiting our experimental timescales to about one hour. For studies of crystallisation, we orient the sample capillaries perpendicular to gravity, mitigating its effect. We note that for this system a disordered layer forms on the capillary walls which inhibits heterogenous nucleation.

We estimate the effect of temperature on the radius of gyration of the polymer as shown in Fig. 1. We use the following expression

$$R_G(T) = R_G^\theta \left[\sqrt{2} \left(1 - \exp \left(\frac{T^\theta - T}{\tau} \right) \right) + 1 \right] \quad (2)$$

for $T \geq T^\theta$ which closely matches experimental data over the relevant temperature range [30]. Here the parameter $\tau = 20^\circ \text{C}$.

2.2. Comparison with theory

As mentioned in the introduction we choose to interpret our experimental results within the framework of the simple AO model. A key ingredient is locating, in the AO phase diagram, the (metastable) fluid-fluid binodal for size- ratios $q \sim 0.2$. There are computer simulation results for the binodal and its critical point for $q = 0.1$ [14, 32] and for $q = 0.15$ [24]. Clearly in both cases $q < 0.1547$ so the mapping to an effective one-component fluid that is described by only the pair potential Eq. (1) is exact. Although our experimental systems have $q \sim 0.2$, within the context of AO we can expect three-body contributions to the effective Hamiltonian to play only a very small role. In order to ascertain the phase behaviour of the AO model it is tempting to turn to the free-volume theory [13, 14] which yields simple recipes for calculating both fluid-solid and fluid-fluid phase equilibria for the binary AO mixture. This approximation is fairly successful for size- ratios $\gtrsim 0.4$. However, for $q = 0.1$ free-volume theory provides a reasonably accurate description of fluid-solid coexistence [14] but is quantitatively poor at describing the metastable fluid-fluid coexistence. Specifically it predicts a critical value of ϕ_p that is in reasonable agreement with simulation but a critical value of $\phi_c \sim 0.57$ that is unphysically large [14].

In Fig. 2 we plot the fluid-fluid spinodal for $q = 0.214$, the value that corresponds to the experimental system at room temperature $T = 25^\circ \text{C}$, calculated from free-volume theory using the analytical expression derived by Schmidt *et al.* [33]:

$$\phi_P = \frac{\theta_1^4 \theta_2 / \phi_c}{\alpha (12\theta_1^3 + 15q\theta_1^2\theta_2 + 6q^2\theta_1\theta_2^2 + q^3\theta_2^3)} \quad (3)$$

where $\theta_1 = (1 - \phi_c)$ and $\theta_2 = (1 + 2\phi_c)$ and α is the free volume fraction [13, 33].

One finds that the critical point is at about $\phi_c = 0.40$, $\phi_p = 0.35$. Once again the critical colloid fraction appears rather high. We shall argue that a more accurate value is $\phi_c \sim 0.27$.

Clearly a more reliable prescription is required to estimate the critical point and therefore the location of the binodal. For models like the present, where attractive interactions are short-ranged (sticky), Vliegenthart and Lekkerkerker [34] and Noro and

Frenkel [35] argued that a useful estimate of the critical temperature (or interaction strength) could be obtained by considering the reduced, with respect to HS, second virial coefficient given by

$$B_2^* = \frac{3}{\sigma^3} \int_0^\infty dr r^2 [1 - \exp(-\beta u(r))] \quad (4)$$

where $u(r)$ is the pair potential. These authors proposed that for a wide class of model fluids $B_2^* \sim -1.5$ at the critical temperature. Later Largo and Wilding [36] carried out simulations for effective (depletion) potentials calculated for additive binary HS systems with size-ratios $q = 0.1$ and 0.05 . For these small ratios the effective pair potentials are similar to the AO potential [Eq. 1] but with an additional repulsive barrier.

For all the potentials they considered, Largo and Wilding found that the value of B_2^* at criticality obtained from simulation was very close to $B_2^{*AHS} = -1.207$, i.e. the value reported for the adhesive hard sphere (AHS) model at its critical point [37]. Ashton applied the same criterion for the AO potential [Eq. (1)] with $q = 0.1$ [32]. He found that his simulation result for the critical reservoir fraction ϕ_p was 0.249 , very close to the value 0.248 given by the B_2^{*AHS} criterion. We also considered the simulation results of Fortini et.al. [24] for the AO model with $q = 0.15$. In this case the critical value of ϕ_p is ~ 0.316 which is again close to the value 0.313 from the B_2^{*AHS} criterion. Since the size-ratios we consider are not vastly larger than those considered above, we chose to estimate the critical value of ϕ_p by calculating B_2^* for the AO potential [Eq. (1)] and employing the B_2^{*AHS} criterion. In order to estimate the critical colloid fraction we used the mapping to the square-well potential proposed by Noro and Frenkel [35] to obtain an effective range. For the three temperatures, i.e. the three q values, that we consider the estimate of the critical colloid fraction is about 0.27 which happens to be equal to the AHS value [37].

It is important to note that the simulations of the AO model, and of other models with short-ranged attraction, report broad, in ϕ_c , gas-liquid coexistence curves extending to large values of ϕ_c and it is clear that extracting an accurate value for the critical colloid fraction can be difficult. Our resulting estimates of the AO model critical points are shown as open squares in Fig. 2 and Fig. 4 where we also sketch putative spinodals. Since our estimates are based on empirical recipes we remark that using the slightly higher value of -1.174 for the critical value of B_2^{*AHS} , reported by Largo et al. [38], makes no discernible difference in our plots. Note also that their revised value of the critical packing fraction for AHS is 0.29 , only slightly bigger than the earlier result for AHS. Moreover were we to employ the original estimate for the critical value of B_2^* , namely -1.5 , we find this results in only minor changes (about 4%) to the critical value of ϕ_p , for the size-ratios relevant for our systems.

3. Results

3.1. Room-temperature behaviour

We begin our presentation of results with the phase diagram at ambient conditions as shown in Fig. 2. Throughout we work in the colloid volume fraction ϕ_c and reservoir polymer number density ρ_p plane. We calculate ρ_p following the free-volume prescription for the AO model [13] : $\rho_p = \rho_p^{exp}/\alpha$, where ρ_p^{exp} is the experimental value for the polymer number density and α is the free-volume fraction entering Eq. (3). In the free-volume approximation, α depends on q and ϕ_c only [14]. For a size-ratio $q \sim 0.2$ and colloid volume fractions up to $\phi_c \sim 0.4$ we expect this approximation to be accurate. Our choice of representation is motivated by two considerations : firstly, polymer number density is conserved during heating and cooling (while polymer “volume fraction” emphatically is not), and secondly, the reservoir representation permits easy visual comparison with theoretical spinodal lines and critical points.

We calculate theoretical phase boundaries as outlined in Section 2.2: fluid-solid coexistence is determined using free volume theory [13] and the metastable fluid-fluid critical point is estimated using the B_2^{*AHs} criterion. Experimentally, along the hard sphere line $\phi_p = 0$ (x -axis in Fig. 2) we find hard sphere crystallisation for $\phi_c > 0.54$. However, upon addition of polymer, we found fluid states around the AO fluid-solid phase boundary and gelation at higher polymer concentration. Only around the estimated AO critical point was a pocket of states found which crystallised on the experimental timescale of 6 days. This is the shaded region in Fig. 2.

We already remarked that the fluid-gelation boundary has been identified with the fluid-fluid spinodal [25, 26]. In Fig. 2 we plot the spinodal calculated from free-volume theory, i.e. Eq. (3), and a sketch of where the spinodal should be located for the AO model, based on our B_2^{*AHs} criterion for the critical point. As mentioned earlier, free-volume theory grossly overestimates the colloid critical fraction for this size-ratio $q = 0.214$ thus in making comparison with experiment it is appropriate to focus on the B_2^{*AHs} result. We observe that the states identified as gels (triangles) all lie within the (putative) AO spinodal. Below the estimated AO fluid-fluid critical point we find only fluid states. We may conclude that the AO critical point provides an excellent indicator of the location of the experimental transition between fluid and gel states at this temperature.

3.2. Critical enhancement of crystallisation

Crystallisation of colloid-polymer mixtures is described in Fig. 3. The crystals formed in the shaded region of Fig. 2 are markedly different from those formed in the absence of polymer in that the fluid is at a much lower colloid packing fraction. Crystallisation times vary from 1 to 6 days. We observe crystallisation only in a small “pocket” around the critical polymer number density $\rho_p^c \sigma^3 \sim 72$.

Some samples which crystallised were fluids prior to freezing (hatched circles in Fig.

2), while some were gels (hatched squares in Fig. 2). That crystallisation is found to occur in the neighbourhood of the (metastable) critical point predicted by our B_2^{*AHs} criterion is remarkable and we explore this aspect further in Fig. 3(c) where we plot the crystallisation time as a function of polymer concentration. The crystallisation time τ_X is the time at which more than 50 % of the sample had crystallised. As seen in Fig. 3(b), crystallisation is rather clear. The unit of time employed is the Brownian time, defined as $\tau_B = \pi\eta\sigma^3/k_BT$, where η is the viscosity and is equal to 0.42 s for this system. We find that in the (metastable) one-phase fluid region, moving further from criticality, the crystallisation time increases rapidly and takes values outside the experimental time-window. This is consistent with the two step nucleation scenario of ten Wolde and Frenkel [27].

3.3. Response to temperature

We now consider the effect of temperature on our system. The results are given in Fig. 4. Using the temperature stage we cool the system to around 10°C. The images in Figs. 4(a-c) show the effect of then gently heating the system. A metastable fluid (a) condenses (b) and finally forms a gel (c). The phase diagrams shown in the main panel pertain to the AO model and are obtained using the same prescriptions as in Fig. 2. It is assumed that the only effect of temperature T is to change the radius of gyration according to Eq. 2 and we calculate the size ratio using $q = 2R_G(T)/\sigma$. We find $q = 0.214, 0.197$ and 0.176 for $T = 25^\circ\text{C}, 15^\circ\text{C}$ and 10°C , respectively. Within the context of the free volume approximation the fluid-solid coexistence lines in the $\phi_c - \phi_p$ plane change little over this range of q and we fixed these to be the lines for $q = 0.18$. It is the scaling with $(\sigma/\sigma_p)^3$, from the polymer volume fraction to the polymer reservoir density, that gives rise to the variation shown in the figure. Although the experimental data show considerable scatter, which we attribute predominantly to sedimentation effects, there is reasonable overall agreement with the theoretical predictions. Specifically we find that a transition from a fluid to a gel as illustrated in Fig. 4 (a-c) occurs at temperatures broadly consistent with the location of the spinodals as predicted by our B_2^{*AHs} criterion. It appears that the assumption of ideal polymer behaviour is a reasonable first step to treating the temperature response of colloid-polymer mixtures.

4. Conclusions

We have examined the room-temperature behaviour of a colloid-polymer mixture and its response to temperature quenches. To the best of our knowledge, these are the first particle-resolved studies of the latter. At ambient conditions, the fluid-gel transition is well described by an estimate of the spinodal based on a second virial coefficient criterion for the effective one-component Asakura-Oosawa model. Although free-volume theory provides a reasonable description of fluid-crystal coexistence, we emphasize that this approximation predicts a spinodal which lies at unphysically large colloid volume

Temperature as an external field for colloid-polymer mixtures : “quenching” by heating and “melting” by cooling
fractions.

The response to temperature is consistent with our assumptions that the polymers can be treated as ideal, and that the radius of gyration follows a simple fit to experimental results [30] [Eq. (2)]. This opens the way to 3D particle-resolved studies of a variety of phenomena related to systems with attractive interactions which are tuneable *in-situ*.

We find crystallisation on observable timescales close to the metastable critical point predicted by our B_2^{*AHs} criterion. Assuming the mapping we have carried out is accurate, we find crystallisation in the metastable one-phase region, on a timescale which increases further from criticality, in addition to the metastable two-phase region. This contrasts with results from Brownian dynamics simulations where crystallisation was found only in the metastable gas-liquid two-phase region [24, 39]. We attribute this to the very much longer timescale accessed in the experiments.

Concerning the lack of crystallisation in the fluid-crystal coexistence regions, a question arises in the apparent discrepancy between our results and Ilett *et al.* [15], who found a closer agreement with the prediction of the fluid-crystal boundary from free volume theory in a comparable system (with size ratio $q = 0.08$). However in their case, the colloid diameter was $\sigma \approx 400$ nm, compared to $\sigma \approx 1080$ nm here. This has drastic consequences for the dynamics of the system, as the time for a colloid to freely diffuse over its own diameter scales with the cube of the particle size. Thus the effective timescales are around 20 times less in this work. Typical crystallisation times were around 6 hours in their case. This corresponds to 120 hours for our systems, which is far beyond the experimental limits imposed by sedimentation of around one hour. Observations such as this underline the challenges for self-assembly in this size range and serve to emphasise the very dependence of timescales in these systems upon colloid size.

Acknowledgments SLT and CPR acknowledge the Royal Society for financial support and EPSRC grant code EP/H022333/1 for provision of the confocal microscope used in this work. Gregory N. Smith is kindly acknowledged for preliminary experiments. It is a pleasure to thank Daan Frenkel and Richard Sear for many stimulating discussions.

References

- [1] W. C. K. Poon. The physics of a model colloid-polymer mixture. *Journal of Physics, Condensed Matter*, 14(33):R859–R880, August 2002.
- [2] H. N. W. Lekkerkerker and R. Tuinier. *Colloids and the Depletion Interaction*, volume 833 of *Lecture Notes in Physics*. Berlin: Springer, 2011.
- [3] S. Asakura and F. Oosawa. On interaction between 2 bodies immersed in a solution of macromolecules. *J Chem Phys*, 22(7):1255–1256, 1954.
- [4] S. Asakura and F. Oosawa. Interaction between particles suspended in solutions of macromolecules. *J. Poly. Sci.*, 33:183–192, 1958.
- [5] B. Vincent. *J. Coll. Interf. Sci.*, 42:545, 1972.
- [6] A. Vrij. Polymers at interfaces and interactions in colloidal dispersions. *Pure Appl. Chem.*, 48(4):471–483, 1976.

- [7] K. N. et. al. Pham. Multiple glassy states in a simple model system. *Science*, 296:104–106, 2002.
- [8] E. H. A. de Hoog, W. K. Kegel, A. van Blaaderen, and H. N. W. Lekkerkerker. Direct observation of crystallisation and aggregation in a phase-separating colloid-polymer suspension. *Phys. Rev. E*, 64:021407, 2001.
- [9] D. G. A. L. Aarts, M. Schmidt, and H. N. W. Lekkerkerker. Direct observation of thermal capillary waves. *Science*, 304:847–850, 2004.
- [10] C. P. Royall, D. G. A. L. Aarts, and H. Tanaka. Bridging length scales in colloidal liquids and interfaces from near-critical divergence to single particles. *Nature Physics*, 9:636–640, 2007.
- [11] J. R. Savage and A. D. Dinsmore. Experimental evidence for two-step nucleation in colloids. *Phys. Rev. Lett.*, 102:198302, 2009.
- [12] A. P. Gast, C. K. Hall, and W. B. Russel. Polymer-induced phase separations in nonaqueous colloidal suspensions. *J. Coll. Interf. Sci.*, 96:251–267, 1983.
- [13] H. N. W. Lekkerkerker, W. C. K. Poon, P. N. Pusey, A. Stroobants, and P. B. Warren. Phase-behavior of colloid plus polymer mixtures. *Europhys. Lett.*, 20(6):559–564, November 1992.
- [14] M. Dijkstra, J. M. Brader, and R. Evans. Phase behaviour and structure of model colloid-polymer mixtures. *J. Phys.: Condens. Matter*, 11:10079–10106, 1999.
- [15] S. M. Ilett, A. Orrock, W. C. K. Poon, and P. N. Pusey. Phase behaviour of a model colloid-polymer mixture. *Phys. Rev. E*, 52:1344–1352, 1995.
- [16] M. Dijkstra, R. van Roij, and R. Evans. Effective interactions, structure, and isothermal compressibility of colloidal suspensions. *J. Chem. Phys.*, 113:4799–4807, 2000.
- [17] C. P. Royall, A. A. Louis, and H. Tanaka. Measuring colloidal interactions with confocal microscopy. *J. Chem. Phys.*, 127(4):044507, 2007.
- [18] A.M. Alsayed, Z. Dogic, and A.G. Yodh. Melting of lamellar phases in temperature sensitive colloid-polymer suspensions. *Phys. Rev. Lett.*, 93:057801, 2004.
- [19] C. Hertlein, L. Helden, A. Gambassi, S. Dietrich, and C. Bechinger. Direct measurement of critical casimir forces. *Nature*, 172-175:451, 2008.
- [20] H. Guo, T. Narayanan, M. Sztuchi, P. Schall, and G. H. Wegdam. Reversible phase transition of colloids in a binary liquid solvent. *Phys. Rev. Lett.*, 100:188203, 2007.
- [21] D. Bonn, J. Otwinowski, S. Sacanna, H. Guo, G. Wegdam, and P. Schall. Direct observation of colloidal aggregation by critical casimir forces. *Phys. Rev. Lett.*, 103:156101, 2009.
- [22] N. Elsner, D. R. E. Snoswell, C. P. Royall, and B. V. Vincent. Simple models for 2d tunable colloidal crystals in rotating ac electric fields. *J. Chem. Phys.*, 130:154901, 2009.
- [23] A. Ivlev, G. Morfill, H. Loewen, and Royall C. P. *Complex Plasmas and Colloidal Dispersions: Particle-Resolved Studies of Classical Liquids and Solids*, volume 5 of *Series in Soft Condensed Matter*. World Scientific Publishing Co., Singapore, 2012.
- [24] A. Fortini, E. Sanz, and M Dijkstra. Crystallization and gelation in colloidal systems with short-ranged attractive interactions. *Phys. Rev. E*, 78:041402, 2008.
- [25] N. A. M. Verhaegh, D. Asnaghi, H. N. W. Lekkerkerker, M. Giglio, and L. Cipelletti. Transient gelation by spinodal decomposition in colloid-polymer mixtures. *Physica A*, 242:104–118, 1997.
- [26] P. J. Lu, E. Zaccarelli, F. Ciulla, A. B. Schofield, F. Sciortino, and D. A. Weitz. Gelation of particles with short-range attraction. *Nature*, 435:499–504, 2008.
- [27] P. R. Ten Wolde and D. Frenkel. Enhancement of protein crystal nucleation by critical density fluctuations. *Science*, 277:1975–1978, 1997.
- [28] O Galkin and P Vekilov. Control of protein crystal nucleation around the metastable liquid-liquid phase boundary. *Proc. Nat. Acad. Sci.*, 97:6277–6281, 2000.
- [29] P. G. Vekilov. Nucleation. *Crystal Growth and Design*, 10:5007–5019, 2010.
- [30] G.C. Berry. Thermodynamic and conformational properties of polystyrene. i. light-scattering studies on dilute solutions of linear polystyrenes. *J. Chem. Phys.*, 44:4550–4564, 1966.
- [31] B. Vincent. The calculation of depletion layer thickness as a function of bulk polymer concentration. *Colloids and Surfaces*, 50:241–249, 1990.
- [32] personal communication. Douglas Ashton.

- [33] M. Schmidt, H. Loewen, J. M. Brader, and R. Evans. Density functional theory for a model colloid-polymer mixture: bulk fluid phases. *J. Phys.: Condens. Matter*, 14:9353–9382, 2002.
- [34] G. A. Vliegenthart and H. N. W. Lekkerkerker. Predicting the gas-liquid critical point from the second virial coefficient. *J. Chem. Phys.*, 112:5364–5369, 2000.
- [35] M. G. Noro and D. Frenkel. Extended corresponding-states behavior for particles with variable range attractions. *J. Chem. Phys.*, 113:2941–2944, 2000.
- [36] J. Largo and N. B. Wilding. Influence of polydispersity on the critical parameters of an effective-potential model for asymmetric hard-sphere mixtures. *Phys. Rev. E*, 73:036115, 2006.
- [37] M.A. Miller and D. Frenkel. Competition of percolation and phase separation in a fluid of adhesive hard spheres. *Phys. Rev. Lett.*, 90:135702, 2003.
- [38] J. Largo, M. A. Miller, and F. Sciortino. The vanishing limit of the square-well fluid: The adhesive hard-sphere model as a reference system. *J. Chem. Phys.*, 128:134513, 2008.
- [39] C. P. Royall and A. Malins. The role of quench rate in colloidal gels. *Cond-Mat: ArXiv*, page arXiv:1203.0664, 2012.

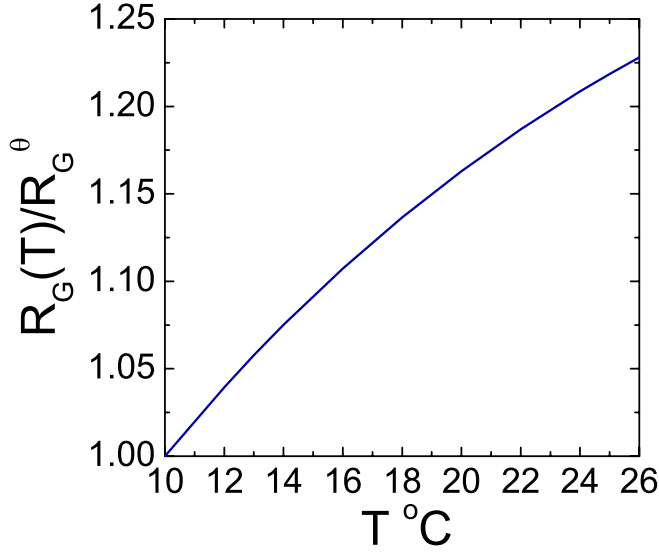


Figure 1. (color online) The radius of gyration R_G of polystyrene. This is a fit, Eq. (2), to experimental data [30].

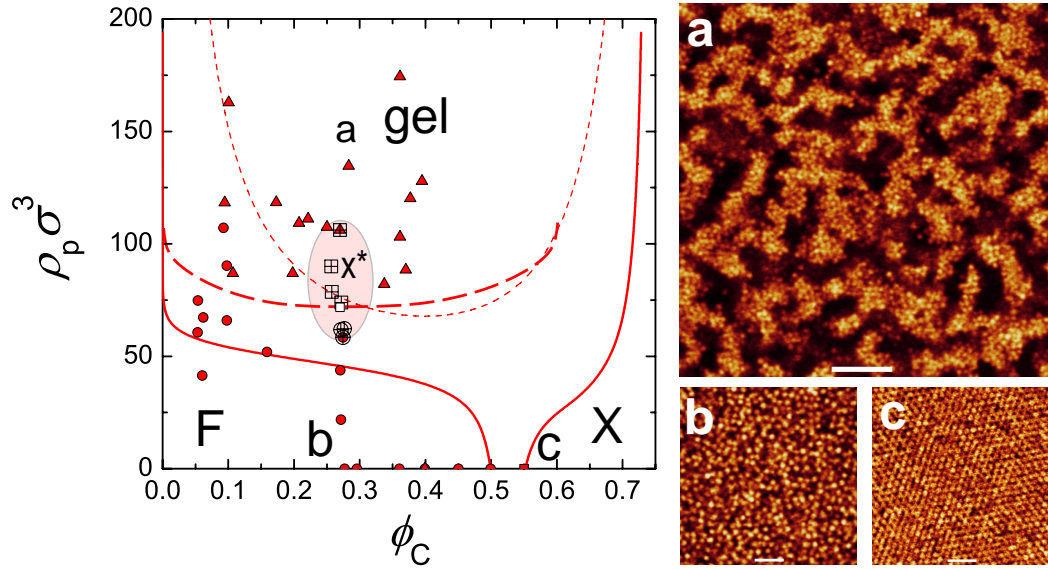


Figure 2. (color online) Phase diagram at room temperature in the colloid volume fraction ϕ_c and reservoir polymer number density ρ_p plane. Symbols are experimental data; circles are fluid (F), triangles are gels and squares are crystals (X). Shaded area marked x^* denotes samples which crystallised on the experimental timescale: hatched squares were initially gels, and hatched circles were initially fluids. The data are compared with theoretical predictions for the AO model with $q = 0.214$ from free volume theory for fluid-solid coexistence (solid lines) [13] and for the liquid-gas spinodal (short-dashed line) (Eq. 3). The unfilled square is the AO critical point according to our B_2^{AHS} criterion and the long dashed line is a sketch of the accompanying spinodal. (a)-(c) are confocal microscopy images of a gel (a), fluid (b) and (hard sphere) crystal (c) at states in the phase diagram shown in the main panel. Bars=20 μm .

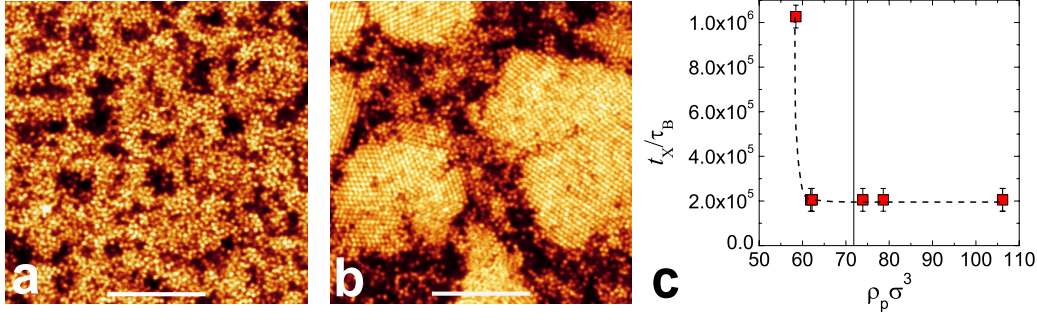


Figure 3. (color online) Crystallisation in colloid-polymer mixtures at room temperature. (a) immediately after preparation, (b) after 1 day. Bars= $20 \mu m$. (c) Crystallisation times in units of the Brownian time τ_B as a function of polymer number density. Vertical line is the critical polymer number density estimated for the AO model, with $q = 0.214$, from the $B_2^{*AH S}$ criterion. Dashed line is a guide to the eye.

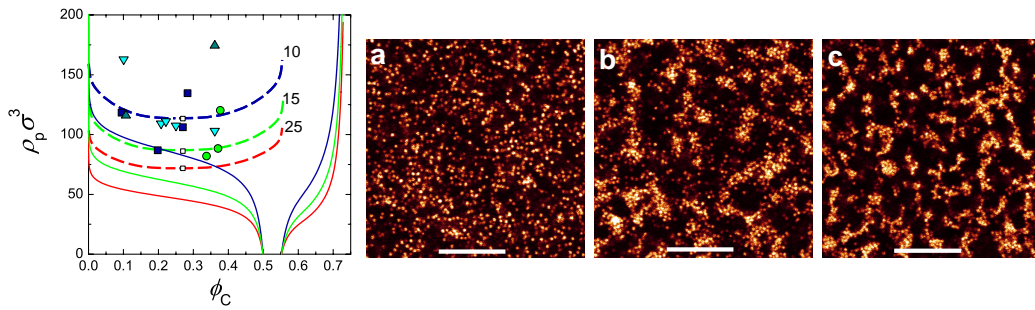


Figure 4. (color online) The fluid-gel transition at different temperatures. (a-c) shows a typical experiment where the transition temperature is found by “quenching” a colloid-polymer mixture by heating. Here $\phi_c = 0.107$ and $\rho_p = 116\sigma^{-3}$. (a) 8.5°C, fluid, (b) 10.2°C condensing, (c) 11.8°C, gel. The transition is then identified as around 10°C. In the main panel, experimental data indicate fluid-gel transitions at 10°C (blue squares), 11°C (turquoise up triangles), 12°C (cyan down triangles) and 16°C (green circles). As in Fig. 2, AO free volume theory fluid-crystal coexistence lines are solid, and critical points (unfilled squares) follow our $B_2^{*AH S}$ criterion with accompanying sketched spinodal (long dashed lines). These are shown for room temperature (25°C), 15°C and 10°C as indicated, corresponding to $q = 0.214$, 0.197 and 0.176, respectively. Bars= $20 \mu m$.